



# Enhanced performance and cost-effectiveness of Pd-based catalysts with Cu, Ni, and Co promoters for CO and NO<sub>x</sub> conversion in flue gas emission

Owais Al-Aqtash<sup>a</sup>, András Sápi<sup>a,\*</sup>, Ferenc Farkas<sup>b</sup>, Haythem S. Basheer<sup>a</sup>,  
Ákos Kukovecz<sup>a</sup>, Zoltán Kónya<sup>a</sup>

<sup>a</sup> University of Szeged, Interdisciplinary Excellence Centre, Department of Applied and Environmental Chemistry, Rerrich Béla tér 1, H-6720, Szeged, Hungary

<sup>b</sup> Department of Technology, Faculty of Engineering, University of Szeged, Mars tér 7, H-6724, Szeged, Hungary

## ARTICLE INFO

### Keywords:

Flue gas conversion  
Catalytic converters  
Metals synergy  
Bimetallic catalytic converters

## ABSTRACT

This study investigates the efficiency and cost-effectiveness of cobalt, nickel, and copper as promoters for palladium catalysts supported on pelletized aluminum oxide, aimed to enhance the performance of catalytic converters for flue gas treatment. We explored the outstanding performance and conversion costs of these transition metals and noble metal catalysts. A series of 12 samples with varying metal loadings were synthesized and evaluated under conditions simulating real driving environments from the automotive world. The flue gas conversion results demonstrated significant improvements in catalytic activity across all promoter-enhanced samples. Notably, the 5 wt% Co + 0.1 wt% Pd combination exhibited a remarkable 38 % increase in CO conversion at 0.5 kW operating condition and a 27 % improvement at 1.0 kW while reducing the cost of conversion by 61 %, compared to the 0.1 wt% Pd benchmark. Regarding NO<sub>x</sub> conversion, Ni/Pd samples showed superior performance, with enhancements of 14 % at 0.5 kW and 36 % at 1.0 kW relative to the pure Pd catalyst. The observed performance enhancements are suggestive of a synergistic effect ... Further surface characterization would be needed to fully elucidate the specific mechanisms involved. Our research highlights the potential for developing more efficient and cost-effective catalytic systems for automotive emissions control through strategic metal combinations.

## 1. Introduction

Catalytic converters are critical components in reducing harmful emissions from internal combustion engines. These devices rely on catalysts, typically composed of noble metals, to facilitate the conversion of toxic exhaust gases like carbon monoxide, hydrocarbons, and nitrogen oxides into less harmful substances such as carbon dioxide, water vapor, and nitrogen. Among noble metals, palladium (Pd), platinum (Pt), and rhodium (Rh) have traditionally been favored due to their high catalytic efficiency. However, the escalating cost and limited availability of these precious metals present significant challenges to both economical and sustainable automotive manufacturing. As a result, recent research has focused on improving catalyst efficiency while reducing the reliance on these scarce materials, with techno-economic and techno-ecological assessments providing a framework to evaluate the overall impact of alternative catalytic systems (Bin et al., 2022; Michalek et al., 2024) In recent years, researchers have increasingly

emphasized techno-ecological assessments, which evaluate the performance of catalytic systems and also their environmental and economic impacts throughout their lifecycle (Uddin and Wang, 2024; Yadav et al., 2023). These assessments highlight the need to reduce noble metal content while maintaining or enhancing catalytic efficiency. This challenge has driven significant interest in transition metals as promoters for noble metal catalysts in automotive applications. Transition metals such as nickel (Ni), cobalt (Co), and copper (Cu) are more abundant and less expensive than noble metals, offering a pathway to reducing costs while maintaining or even enhancing catalytic performance. Studies show that the incorporation of transition metals can also improve the catalyst's resistance to poisoning, a critical factor in the long-term durability and sustainability of catalytic converters (Darby et al., 2018; Robles-Lorite et al., 2023).

Recent literature has demonstrated that the combination of noble metals with transition metals in bimetallic systems can create a synergistic effect, improving both catalytic activity and stability. For instance,

\* Corresponding author.

E-mail address: [sapia@chem.u-szeged.hu](mailto:sapia@chem.u-szeged.hu) (A. Sápi).

<https://doi.org/10.1016/j.apr.2025.102579>

Received 30 September 2024; Received in revised form 9 May 2025; Accepted 10 May 2025

Available online 14 May 2025

1309-1042/© 2025 Turkish National Committee for Air Pollution Research and Control. Published by Elsevier B.V. This is an open access article under the CC BY license (<http://creativecommons.org/licenses/by/4.0/>).

nickel has been widely studied as a promoter for palladium catalysts. Research has shown that adding nickel to palladium can significantly enhance the oxidation of methane, a critical component of hydrocarbon emissions. This synergistic interaction between nickel and palladium not only boosts catalytic activity but also increases resistance to thermal degradation, a common issue in automotive exhaust systems (Choyo et al., 2021, 2022; Xiong et al., 2021; Zou et al., 2017). Similarly, cobalt has been extensively investigated as a promoter for platinum-based catalysts, particularly in the context of CO oxidation. Studies indicate that cobalt enhances catalytic activity and increases the catalyst's resistance to sulfur poisoning, a major challenge for automotive catalytic converters operating in environments with high sulfur content. This increased sulfur tolerance extends the lifespan of the catalyst and improves its overall efficiency in real-world driving conditions (Lin et al., 2022; Zhong et al., 2021a, 2021b). Copper, another promising transition metal, has also shown potential when combined with palladium for NOx reduction. Recent research has demonstrated that copper-promoted palladium catalysts outperform conventional systems in the reduction of NOx, CO, and hydrocarbons. The addition of copper not only improved catalytic efficiency but also contributed to a reduction in the overall palladium content, aligning to reduce the environmental and economic costs associated with noble metals (Kim et al., 2018; Li et al., 2021; Peckmann, 2021; King et al., 2019). Several techno-economic analyses have underscored the potential for transition metal promoters to reduce the reliance on costly noble metals in catalytic converters. These studies emphasize that the adoption of bimetallic catalysts can significantly lower the overall material costs of catalytic converters while maintaining or enhancing emission control performance (Beobide et al., 2022; Guzzi et al., 2010; Liu and Corma, 2023; Nazarpour and Golden, 2016; Salaev et al., 2022). Moreover, from an ecological standpoint, transition metals are more abundant and less environmentally destructive to mine than noble metals, making them a more sustainable option in the long term. This aligns with global efforts to reduce the ecological footprint of vehicle manufacturing and operation, particularly in light of increasingly stringent emission regulations (Nkuna et al., 2022; Padamata et al., 2020). In conclusion, the integration of transition metals such as nickel, cobalt, and copper as promoters in palladium-based catalytic systems presents a promising strategy for enhancing the performance and cost of automotive catalytic converters.

Despite these advancements, there remains a gap in understanding how these promoters perform under real driving conditions and across different engine operating parameters. Additionally, a direct comparison of the cost-effectiveness of copper, nickel, and cobalt as promoters for palladium catalysts in a single study has not been thoroughly explored. The main objective of this experiment was to address these knowledge gaps by exploring the synergy between cheap and noble metals, specifically focusing on improving the performance of catalytic converters used in gasoline vehicles. The research investigated the addition of cobalt, nickel, and copper as promoters for palladium catalysts supported on pelletized aluminum oxide under simulated real driving conditions. This study aims to contribute to the ongoing efforts to develop more efficient and cost-effective catalytic converters, potentially reducing emissions and lowering production costs for automotive emission control systems.

## 2. Experimental methods & materials

### 2.1. Materials

- Palladium (II) acetate ( $\text{Pd}(\text{OCOCH}_3)_2$ ;  $\geq 97\%$ , Sigma Aldrich)
- Nickel (II) acetylacetonate ( $\text{C}_{10}\text{H}_{14}\text{NiO}_4$ ;  $\text{Ni} \geq 98\%$ , Merck KGaA)
- Copper (II) acetate monohydrate ( $\text{C}_4\text{H}_6\text{CuO}_4 \cdot \text{H}_2\text{O}$ ;  $\text{Cu} \geq 98\%$ , VWR)
- Cobalt (II) acetate tetrahydrate ( $\text{C}_4\text{H}_6\text{CoO}_4 \cdot 4\text{H}_2\text{O}$ ;  $\text{Co} \geq 99\%$ , Fluka)
- Acetone ( $\text{C}_3\text{H}_6\text{O}$ , 99.5 %, VWR)

- Ethanol ( $\text{C}_2\text{H}_5\text{O}$ , purity  $\geq 98\%$ , VWR)
- Distilled water
- The fuel used was commercial unleaded gasoline compliant with EN 228 standards (95 RON,  $\leq 10$  ppm sulfur), composition table (hydrocarbons: 35 % aromatics, 22 % olefins, 43 % paraffins; oxygenates: 3 % ethanol)

Gamma-Aluminum Oxide ( $\text{Al}_2\text{O}_3 \geq 93$ ) was manufactured by Thermo Fischer Scientific under the product name Aluminum oxide, catalyst support, high surface area, Thermo Scientific Chemicals with pellet form of diameter of 1/8" and 0.6 ml/g pore volume.

Structural steel – S235JR-based reaction chamber was built to EN10025 European Production standards. This non-alloy structural steel comprises 0.17 % carbon and has a tensile strength of 400–500 N/mm<sup>2</sup>. The electrical resistance is 0.14  $\Omega\text{mm}^2/\text{m}$ , while the thermal conductivity is 54 W/(m\*K). Figs. 1 and 2 shows the reaction chamber design and the schematic view of the experimental setup, respectively.

### 2.2. Experimental methods

#### 2.2.1. X-ray diffraction (XRD)

The composition of the samples was determined at each step of the project process using a Cu anode X-ray source, for increased resolution the samples were evaluated at a measurement speed of 1°/min. The X-ray diffractometer brand is Rigaku MiniFlex II.

#### 2.2.2. Flue-gas conversion

A Real Driving Emission (RDE) setup was utilized to perform the necessary tests on the prepared samples. The system comprises two primary components: a controlled flue-gas emission source and a gas analyzer. The first is a mobile design measuring table on wheels with a galvanized surface and a damage-prevention frame. The load unit is a three-phase asynchronous electric motor serving as the internal combustion engine's starter. The HONDA GX390 engine is a 4-stroke single-cylinder gasoline engine with a net power of 8.7 KW. The ENERGO-POWER (Telj-4) measurement software, which also regulates the operation of substantial braking systems, can be used to set the static working point or control the entire measuring cycle. All tests were performed at two different engine working conditions (Table 1). The second component is a gas analyzer probe of the testo type, where two sensors are used to read the data before and after the reaction chamber where the prepared samples reside. Each sample was tested at least 3 times at every operating condition, where every test lasted for an average of 1 h. The presented results constitute the average of the collected data. These power levels represent low and medium load conditions for the specific engine used, allowing evaluation under diverse thermal and flow conditions relevant to engine operation.

#### 2.2.3. Preparation of the samples

The list of resulting samples that were prepared during this experiment is listed in Table 2 below. Hereafter the prepared samples are referred to by their short name as listed in the same table.

Each prepared patch contained 100 g of ceramic support before loading it with metals. All catalyst samples were prepared using the wet impregnation method to form a wash-coat covering the ceramic support. Starting with the Ni and Ni/Pd Samples, the impregnating solution is made by dissolving Ni (II) acetylacetonate in distilled water using a stirrer at 40 °C with 500 rpm for 6 h, when the solution was ready, a dropper was used to impregnate the ceramic support with it.

Once the ceramic support completely absorbed the solution, it was then treated in an oxidation furnace with air at 400 °C for 4 h, afterward the sample was wet impregnated with 0.1 wt% Pd, and finally, the resulting samples were treated first in an oxidation furnace with air at 400 °C for 4 h, and second, in a reduction furnace with an H-Ar mixture at 750 °C for 12 h. The Cu, Cu/Pd, Co, and Co/Pd samples followed the same process of preparation except they were dissolved in their suitable

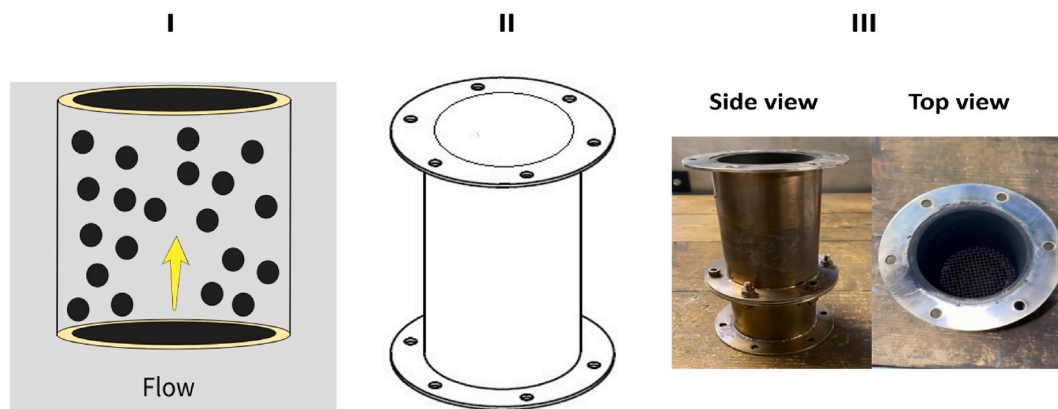


Fig. 1. Reaction chamber used for testing the prepared catalyst where I. shows the schematic emission flow inside the reactor, II. A schematic representation, and III. Shows real photos of the reactor.

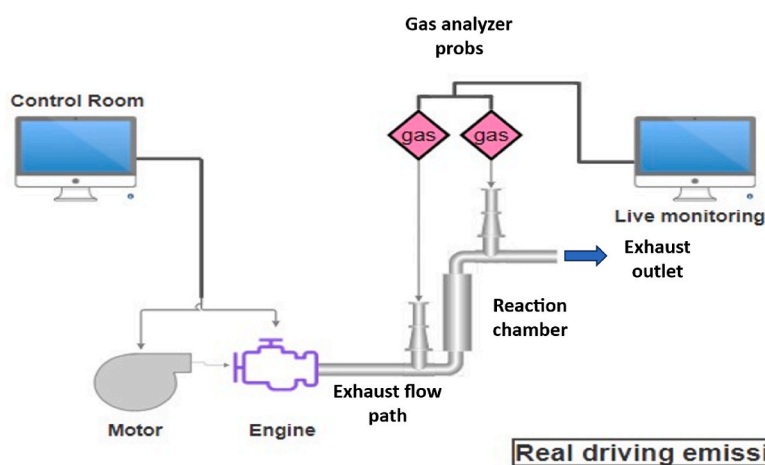


Fig. 2. Schematic representation of the RDE setup utilized for testing the prepared samples.

Table 1

The exhaust flow and engine parameters at the two operating conditions.

|                  | Engine operating Parameters |              |            | Inlet flow parameters |                          |            |
|------------------|-----------------------------|--------------|------------|-----------------------|--------------------------|------------|
|                  | Rpm                         | Torque (n.m) | Vel. (m/s) | Temp. (°C)            | Flow (m <sup>3</sup> /h) | Vel. (m/s) |
| 0.5 kW condition | 2000                        | 2–2.5        | 0.45–0.5   | 500                   | 11000                    | 3.7        |
| 1.0 kW condition | 2000                        | 4.5–5        | 0.95–1     | 590                   | 18000                    | 6.5        |

Table 2

List of the prepared samples and their short names.

|                       | Short name |
|-----------------------|------------|
| 0.1 wt% Pd            | Pd         |
| 1 wt% Cu              | 1 % Cu     |
| 1 wt% Ni              | 1 % Ni     |
| 1 wt% Co              | 1 % Co     |
| 1 wt% Cu + 0.1 wt% Pd | 1 % Cu/Pd  |
| 1 wt% Ni + 0.1 wt% Pd | 1 % Ni/Pd  |
| 1 wt% Co + 0.1 wt% Pd | 1 % Co/Pd  |
| 2 wt% Cu + 0.1 wt% Pd | 2 % Cu/Pd  |
| 2 wt% Ni + 0.1 wt% Pd | 2 % Ni/Pd  |
| 2 wt% Co + 0.1 wt% Pd | 2 % Co/Pd  |
| 5 wt% Cu + 0.1 wt% Pd | 5 % Cu/Pd  |
| 5 wt% Ni + 0.1 wt% Pd | 5 % Ni/Pd  |
| 5 wt% CO + 0.1 wt% Pd | 5 % Co/Pd  |

solvent. Fig. 3 represents some batches of the prepared catalysts.

#### 2.2.4. Energy-Dispersive X-ray Spectroscopy (EDS)

The elemental composition and distribution of the prepared catalysts were analyzed using Energy-Dispersive X-ray Spectroscopy (EDS), EDS measurements were performed at multiple points on the catalyst surface to ensure representative data. The analysis quantified the weight percentages of Cu, Co, Ni, and Pd on the Al<sub>2</sub>O<sub>3</sub> support, verifying the metal loadings achieved through wet impregnation.

### 3. Results & discussion

#### 3.1. Crystal structure analysis (XRD)

The crystallographic structure and phase purity of the prepared materials were determined through XRD pattern and recorded with  $2\theta$  in the range of 4–85° with type X-Pert Pro MPD, Cu-K $\alpha$ :  $\lambda = 1.54 \text{ \AA}$ . Fig. 4 displays characteristic diffraction peaks corresponding to the  $\sim 22.12^\circ$ : Close to the (110)°,  $38.12^\circ$ : Matches with the (222)  $46.27^\circ$ : Near the (400),  $53.64^\circ$ : Matches closely with the (334),  $71.86^\circ$ : Near the (308) and  $79.61^\circ$ : Close to the (533) plane have appeared. It is. These values correspond exactly to the International Center of Diffraction Data ICDD database pattern gamma-alumina JCPDS reference no. 00-010-0425 (gamma-Al<sub>2</sub>O<sub>3</sub>) (Ding et al., 2018; Farahmandjou and Nazafarin, 2015).

These peaks provide clear identification of the crystalline Alumina phase. The Cu & Cu/Pd wet impregnated to Alumina support. No clear peaks appeared for 1 %Cu/Pd, 2 % Cu/Pd, and 5 % Cu/Pd. Also, The Co

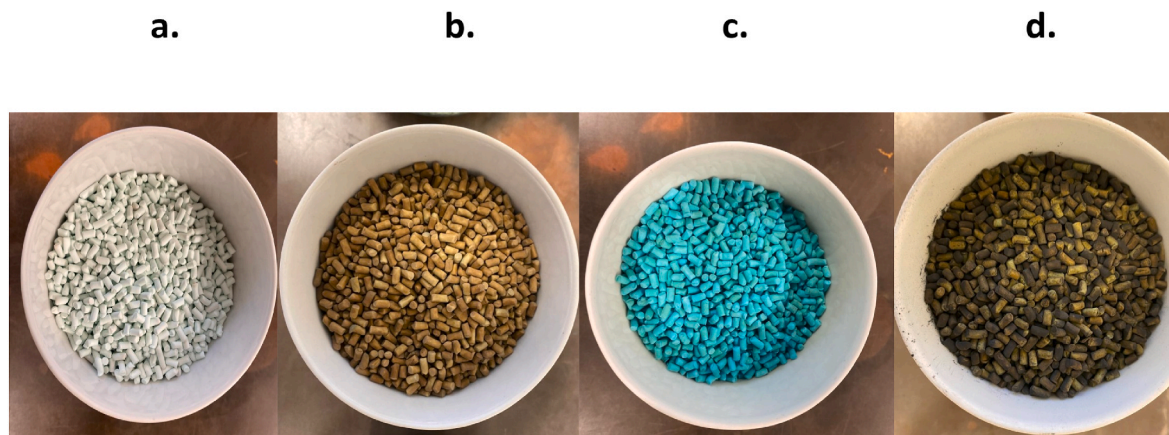


**Fig. 3.** Pictures of the prepared catalysts where **a.** shows Aluminum Oxide support without loadings, **b.** shows a Ni/Pd sample, **c.** shows a Co/Pd sample, and **d.** shows a Cu/Pd sample.

& Co/Pd wet impregnated to Alumina support no clear peaks appeared for 1 %Co/Pd, 2 % Co/Pd, 5 % Co/Pd, and Ni & Ni/Pd wet impregnated to Alumina support no clear peaks appear Cu, Co, and Ni promoted Pd at the Alumina support through wet impregnation, retains the phase structure with enhanced dispersion.

This introduction of the mentioned elements doesn't induce phase changes., only at higher doping levels, showing no new secondary phases (Rezaei and Moradi, 2018). Particle size increases with higher Cu, Co, and Ni loading. The Primary crystallite sizes were calculated using the Scherrer formula in Table 3. Generally, All three systems show similar peak positions, indicating that Pd dominates the crystal structure, peak intensities generally increase with metal loading (1 %–5 %), the oxidized samples consistently show less pronounced peaks across all systems, and finally the "spent" catalysts often show sharper peaks, which could indicate particle growth during use.

### 3.2. Elemental composition analysis (EDS)

To further characterize the catalysts, Energy-Dispersive X-ray Spectroscopy (EDS) was employed to confirm the elemental composition and distribution of Cu, Co, Ni, and Pd on the  $\text{Al}_2\text{O}_3$  support. The results, summarized in Table SM8 in the supplementary material, show that the metal loadings are close to the nominal values, indicating good control over the wet impregnation process. For Cu–Pd catalysts, Cu content increased from 0.9 to 5.6 wt% as the nominal Cu loading rose from 1 % to 5 %, with Pd content ranging from 0.4 to 0.53 wt%. In Co–Pd catalysts, Co varied from 1.0 to 5.7 wt%, with Pd between 0.43 and 0.5 wt%. For Ni–Pd catalysts, Ni content ranged from 0.7 to 6.0 wt%, with Pd from 0.4 to 0.46 wt%. Notably, Pd loadings were consistently higher than the intended 0.1 wt%, which may be attributed to the limitations in EDS sensitivity, or interactions with the support or secondary metals (Cu, Co, Ni), potentially leading to alloy formation or encapsulation. Such interactions could enhance the synergistic effects observed in CO and NO<sub>x</sub> conversion. While EDS verifies elemental incorporation, additional techniques like SEM or XPS could further elucidate surface morphology and chemical states to fully explain the enhanced catalytic activity. Future work will include these methods to confirm the mechanisms underlying the observed synergy.

### 3.3. Flue-gas conversion & cost analysis

We opted to utilize a real driving emission (RDE) setup for testing our sample instead of only using a fixed bed reactor setup due to the nature of this experiment, this was inspired by The European Union (EU) which regulates the emissions limits through the Fuel Quality Directive (FQD) and the European standard EN 228, as they found out that real-world on-

road emissions may be different than the laboratory tests, and the Euro 6 standard in particular, introduced RDE testing to address discrepancies between laboratory tests and on-road performance.

The synergy between transition metals and Pd likely arises from electronic modifications, as Co, Ni, and Cu may donate electrons to Pd, lowering the activation energy for CO and NO<sub>x</sub> reactions, which aligns with the observed conversion trends (Figs. 5 and 6). Promoter metals such as Cu, Ni, and Co play a crucial role in enhancing the catalytic performance of Pd-based systems by modifying electronic properties, enhancing oxygen storage capacity, and providing additional active sites for NO<sub>x</sub> and CO reduction. These modifications lead to improved catalytic activity and selectivity, making these systems highly effective for environmental catalysis applications (Meng et al., 2020; Qi et al., 2024; Salaev et al., 2021; Zhou et al., 2023).

#### 3.3.1. CO conversion

The results of Cu samples show a slight promotion of the catalytic activity toward CO, 1 % Cu/Pd catalyst was able to promote CO conversion by 5 %, whereas 2 % Cu/Pd increased the conversion by 7 % compared to Pd catalyst (Fig. 5.). However, the continuous addition of Cu decreased the CO conversion, particularly at 5 % Cu/Pd where the conversion started dropping. Ni samples showed a unique behavior while converting CO, and although all Ni loading points were able to promote the catalytic activity of the catalyst, increased loading of Ni started dipping the catalyst activity and that is apparent at 5 % Ni/Pd catalyst. Lastly, the Co/Pd samples were the highlight of this experiment as the conversion of CO kept on increasing with the increase of Co loading. The highest loading of Co was 5 % for the sake of consistency of the experiment.

Fig. 5 also present a compelling economic perspective on various palladium-based catalysts, at 0.5 kW and 1.0 kW operating conditions, we observe significant variations in the money spent per 100 ppm CO reduction across different catalyst compositions. However, the 5 %Co/Pd catalyst emerges as the standout performer, achieving the highest conversion rates (55 % and 93 %) while also being the most cost-effective option. Moreover, The overall money spent per 100 ppm reduction at 0.5 kW operating condition is generally lower compared to the 1.0 kW scenario, Lastly, Catalysts like 1 %Ni/Pd, 2 %Cu/Pd, and 2 % Co/Pd present moderate costs and conversion rates, offering a second to best alternative option see Table 4 at the end of this section.

#### 3.3.2. NO<sub>x</sub> conversion

It is important to note that our 'NO<sub>x</sub> conversion' data represents the total reduction of NO and NO<sub>2</sub> species from the gas stream, as measured by our analyzer. We were not able to quantify the specific nitrogen-containing products, such as inert N<sub>2</sub> or nitrous oxide (N<sub>2</sub>O), in this

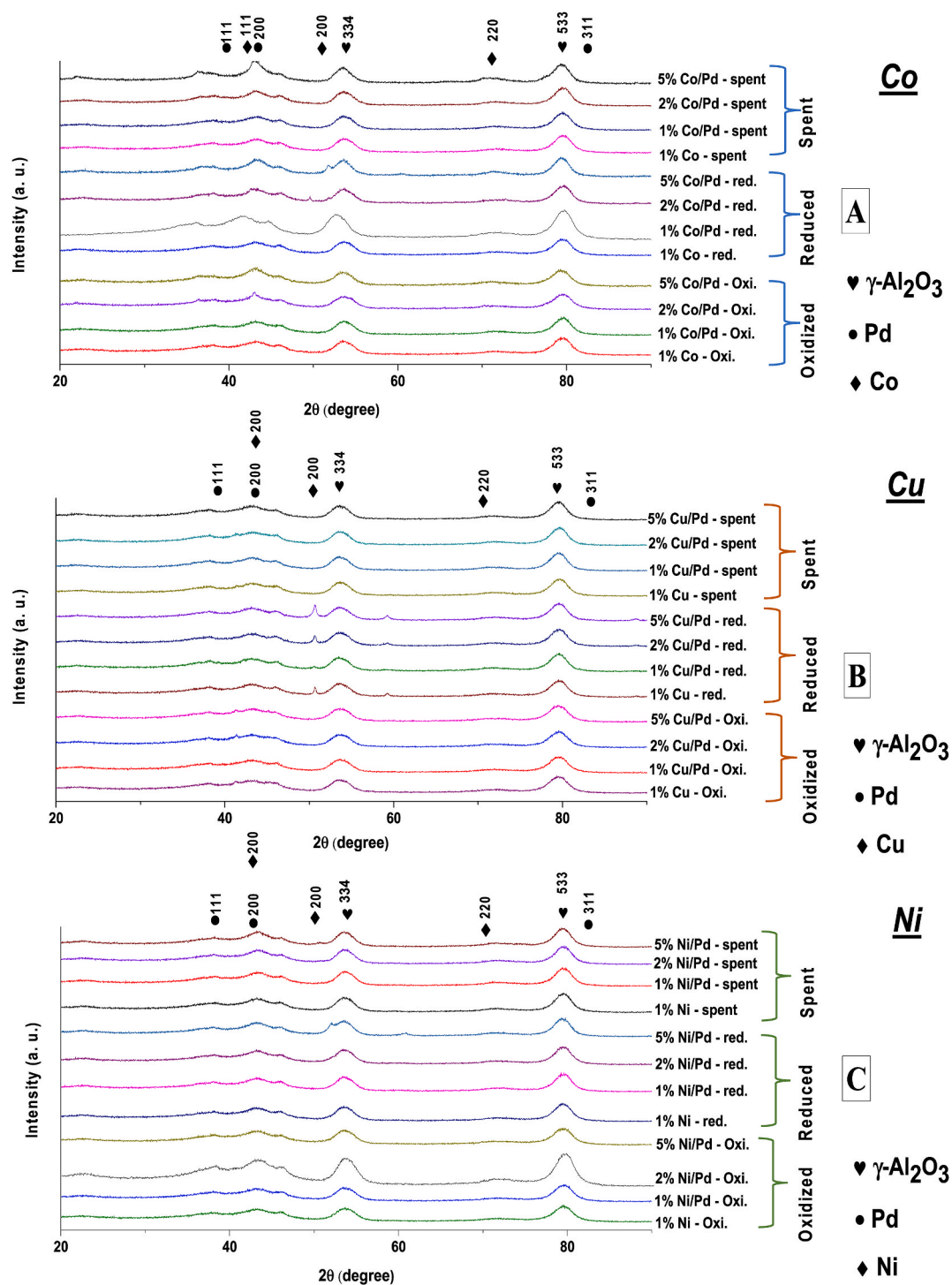


**Fig. 4.** X-ray diffraction patterns of self-prepared A. Co/Pd catalyst, B. Cu/Pd catalyst, and C. Ni/Pd catalyst, all wet impregnated over pelletized  $\text{Al}_2\text{O}_3$  support at 3 different points oxidized at 450 °C for 4 h (fixed temp, no heat rate), reduced in H-Ar mixture at 700 °C for 12 h (heating rate of 5 °C/min), and spent in RDE setup.

study." Because Pt is not as active for NO reduction, commercial catalytic converters use a mixture of noble metals, such as Pt-Pd, rather than solely Pd (Bourges et al., 1998; Després et al., 2004; Kim et al., 2011). Graham et al. reported that Pd functions as a promoter for Pt in the NO conversion process, reducing the hydrothermal sintering of Pt (Graham et al., 2007), from the results it was noticed that Pd catalyst had a moderate  $\text{NO}_x$  conversion, however, the addition of promoters increased the conversion of  $\text{NO}_x$  particles. Fig. 6 shows  $\text{NO}_x$  Conversion and conversion cost for different catalyst compositions at two engine operating conditions mentioned earlier 0.5 kW and 1.0 kW.

In summary, the conversion rates and conversion costs of the different samples are compared to the benchmark conversion of the Pd catalyst which are 73 % and 0.71\$ at the 0.5 kW operating conditions and 28 % and 0.49\$ at 1.0 kW. Results suggest that for all metal types, adding Pd generally improves  $\text{NO}_x$  conversion, especially at higher power. However, the 0.5 kW setting consistently outperforms the 1.0 kW setting across all catalyst types and that is due to the low amounts of  $\text{NO}_x$  produced at this operating condition which averages around 380 ppm compared to 1400 ppm at 1.0 kW operating condition. A limitation of this study is the lack of direct measurement of  $\text{N}_2$  selectivity due to

**Table 3**  
Cu, Co, Ni, and Pd loaded Al<sub>2</sub>O<sub>3</sub> structural parameters.

| Sample (533) hkl | Primary particle Size (nm) |
|------------------|----------------------------|
| 1 % Cu           | 45.22                      |
| 1 % Cu/Pd        | 45.46                      |
| 2 % Cu/Pd        | 45.70                      |
| 5 % Cu/Pd        | 46.20                      |
| 1 % Co           | 45.21                      |
| 1 % Co/Pd        | 45.36                      |
| 2 % Co/Pd        | 35.65                      |
| 5 % Co/Pd        | 46.18                      |
| 1 % Ni           | 45.21                      |
| 1 % Ni/Pd        | 45.33                      |
| 2 % Ni/Pd        | 45.60                      |
| 5 % Ni/Pd        | 46.17                      |

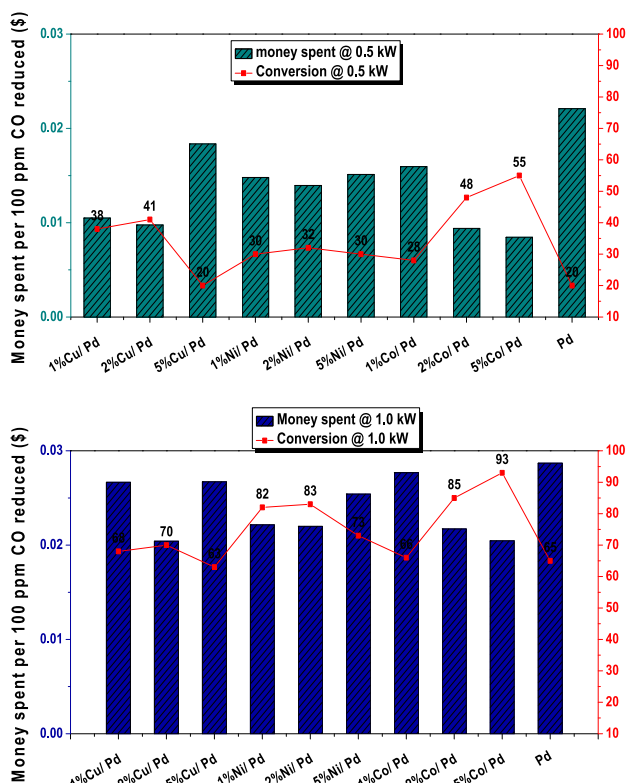


**Fig. 5.** CO conversion and conversion cost results over Cobalt, Copper, and Nickel samples (1 %, 2 %, and 5 %) compared with CO conversion over Pd catalyst samples without promoter addition, at 0.5 and 1.0 kW engine power output operating conditions.

equipment constraints. While literature suggests Pd-based catalysts typically achieve >90 % N<sub>2</sub> selectivity for NO<sub>x</sub> reduction (Graham et al., 2007), the introduction of Cu, Ni, and Co may influence by-product formation, such as N<sub>2</sub>O. Future studies should quantify N<sub>2</sub> and N<sub>2</sub>O to confirm selectivity. The best-performing catalysts at 0.5 kW are 5 % Co/Pd, 2 % Cu/Pd, and 1 % Ni/Pd, whereas at 1.0 kW, the Ni-based catalysts seem to maintain higher conversion rates compared to Co and Cu. Starting with Cobalt-based catalysts, Generally, the 0.5 kW operating condition yields higher NO<sub>x</sub> conversion than 1.0 kW, and the 5 % Co/Pd catalyst shows the highest conversion at 0.5 kW, reaching about 80 %. The Copper-based catalysts showed the same trend of higher conversion at 0.5 kW, where 2 % Cu/Pd shows the best performance at 0.5 kW, with over 80 % conversion, similar to Co adding Pd to Cu significantly improves performance, especially at higher power. Lastly, for Nickel-based catalysts, the 0.5 kW vs 1.0 kW trend persists as 1 % Ni/Pd shows the highest conversion at 0.5 kW, slightly above 80 %.

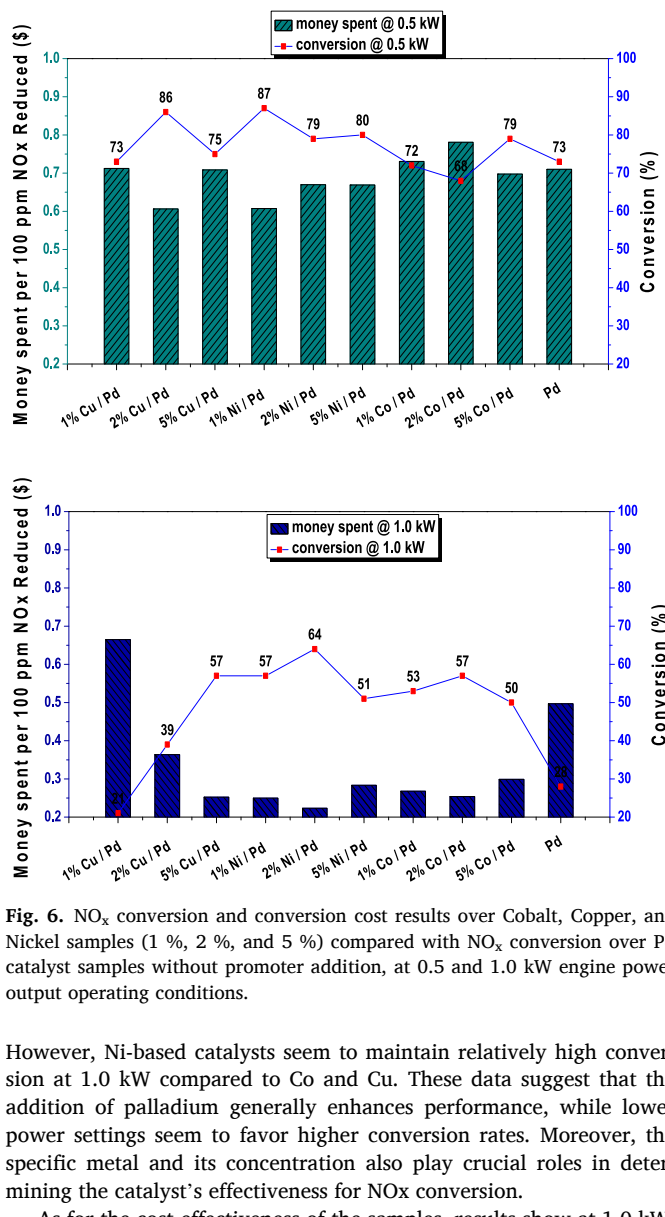


**Fig. 6.** NO<sub>x</sub> conversion and conversion cost results over Cobalt, Copper, and Nickel samples (1 %, 2 %, and 5 %) compared with NO<sub>x</sub> conversion over Pd catalyst samples without promoter addition, at 0.5 and 1.0 kW engine power output operating conditions.

However, Ni-based catalysts seem to maintain relatively high conversion at 1.0 kW compared to Co and Cu. These data suggest that the addition of palladium generally enhances performance, while lower power settings seem to favor higher conversion rates. Moreover, the specific metal and its concentration also play crucial roles in determining the catalyst's effectiveness for NO<sub>x</sub> conversion.

As for the cost-effectiveness of the samples, results show at 1.0 kW, there's a wide range in cost-effectiveness. Some catalysts (like 5 % Cu/Pd) offer high conversion rates at relatively low costs, while others (like pure Pd) are expensive with moderate performance. At 0.5 kW, the cost spread is narrower, but significant differences remain. 5 %Co/Pd stands out as highly cost-effective, offering the highest conversion rate at a moderate cost. It was also evident that changing operating condition from 1.0 kW to 0.5 kW significantly decreases the money spent per 100 ppm NO<sub>x</sub> reduced for all catalysts (by roughly a factor of 20–30), however, this cost reduction comes at the expense of lower conversion rates for most catalysts. So the general conclusion of the financial analysis indicates that first, for high conversion requirements, operating at 1.0 kW with 5 % Cu/Pd catalyst appears to offer the best balance of cost and performance. As For more cost-sensitive applications, operating at 0.5 kW with 5 %Co/Pd catalyst provides excellent cost-effectiveness while maintaining good conversion rates. Pure Pd catalysts are generally not recommended due to their high cost and moderate performance. Doped catalysts offer superior value. Table 4 below provides a comparison of the cost reduction/increase for reducing CO and NO<sub>x</sub> molecules compared with palladium catalyst. The percentages indicate how much each catalyst increased or decreased the cost of conversion relative to the Pd sample at two operating conditions 1.0 kW and 0.5 kW.

**Table 4**Percentages of the decreased cost of CO conversion, and the percentages of the increased/decreased cost of NO<sub>x</sub> conversion all compared to the Pd sample.

|              | CO Conversion Cost |         |         |         |         |         | NO <sub>x</sub> Conversion Cost |         |         |         |        |         |
|--------------|--------------------|---------|---------|---------|---------|---------|---------------------------------|---------|---------|---------|--------|---------|
|              | Cu                 |         | Ni      |         | Co      |         | Cu                              |         | Ni      |         | Co     |         |
|              | 1.0 kW             | 0.5 kW  | 1.0 kW  | 0.5 kW  | 1.0 kW  | 0.5 kW  | 1.0 kW                          | 0.5 kW  | 1.0 kW  | 0.5 kW  | 1.0 kW | 0.5 kW  |
| 1 % pro./ Pd | -7.10 %            | -52.4 % | -22.8 % | -33 %   | -3.60 % | -27.9 % | 33.7 %                          | 0.3 %   | -49.7 % | -14.4 % | -46 %  | 3 %     |
| 2 % pro./ Pd | -28 %              | -55 %   | -23.3 % | -36.9 % | -24.3 % | -57.5 % | -27 %                           | -14.6 % | -55 %   | -5.7 %  | -49 %  | 10 %    |
| 5 % pro./ Pd | -6.90 %            | -16.9 % | -11.5 % | -31.6 % | -28.8 % | -61.7 % | -49 %                           | -0.2 %  | -43 %   | -5.8 %  | -40 %  | -1.70 % |

#### 4. Conclusion

This study examined the effects of different promoters (Cu, Ni, and Co) at various concentrations (1 %, 2 %, and 5 %) on Pd catalysts for CO and NO<sub>x</sub> conversion in flue gas. The performance and cost-effectiveness of these catalysts were compared to a pure Pd sample, the tests were performed in a Real driving Emission setup at two operating conditions (1.0 kW and 0.5 kW). The findings demonstrate significant potential for enhancing catalytic converter performance while reducing noble metal content. The key results are mainly shown in the ability of all samples to promote the catalytic activity of the Pd catalyst although in different percentages. Notably, the 5 wt% Co + 0.1 wt% Pd sample showed the highest conversion of the overall emissions at an average of 93 %, which translates to a 38 % increase while being the most cost-effective sample with a 61.7 % decrease in conversion cost compared to pure Pd catalyst. The observed enhanced performance between palladium and transition metal promoters, particularly cobalt offers promising avenues for developing more efficient and cost-effective catalytic converters. While our study provides valuable insights, it also highlights areas for further investigation. Our experimental results suggest that the enhanced performance of the 5 % Co/Pd catalyst (55.20 % at 0.5 kW) may be attributed to improved dispersion of Pd nanoparticles on the alumina support, as indicated by the XRD analysis (Fig. 4). The observed crystallite size increase with higher Co loading (Table 3) likely facilitates better interaction between Co and Pd, enhancing active site availability for CO oxidation. Additionally, the high NO<sub>x</sub> conversion of Ni/Pd samples (e.g., 87 % at 0.5 kW for 1 % Ni/Pd, Fig. 6) could be due to Ni's ability to modify Pd's electronic properties, promoting NO<sub>x</sub> reduction, as observed in the increased conversion rates compared to pure Pd.

Future research should explore loading optimization, especially for cobalt samples as performance kept increasing with higher loading percentages. Additionally, investigating N<sub>2</sub> selectivity through gas chromatography or mass spectrometry would provide a more comprehensive evaluation of NO<sub>x</sub> conversion efficiency, addressing potential by-product formation like N<sub>2</sub>O. Moreover, I strongly suggest the exploration of a mixture of noble metals particularly Pd and Pt with cobalt promoters to have a better conversion of all flue gas emission components, we also encourage investigation of stability and activity over extended periods. Overall, the addition of promoters generally improved both the performance and cost-effectiveness of the Pd catalyst for flue gas conversion. However, the optimal promoter, concentration, and power level varied between CO and NO<sub>x</sub> conversion. This suggests that the choice of catalyst composition should be tailored to the specific target pollutant and operating conditions.

#### CRedit authorship contribution statement

**Owais Al-Aqtash:** Writing – original draft, Methodology, Investigation, Data curation. **András Sápi:** Writing – review & editing, Supervision, Project administration, Investigation, Funding acquisition. **Ferenc Farkas:** Validation, Investigation, Formal analysis, Data curation. **Ákos Kukovecz:** Resources, Project administration, Funding acquisition, Conceptualization. **Zoltán Kónya:** Supervision, Resources,

Project administration, Methodology, Funding acquisition.

#### Declaration of competing interest

The authors declare that they have no known competing financial interests or personal relationships that could have appeared to influence the work reported in this paper.

#### Acknowledgement

AS gratefully acknowledges the support of FK 143583 and ZK is grateful for K\_21 138714 and SNN\_135918 project from the source of the National Research, Development and Innovation Fund. The Ministry of Human Capacities through the 20391-3/2018/FEKUSTRAT, as well as Project no. TKP2021-NVA-19 under the TKP2021-NVA funding scheme of the Ministry for Innovation and Technology are acknowledged. Project no. RRF-2.3.1-21-2022-00009, titled National Laboratory for Renewable Energy has been implemented with the support provided by the Recovery and Resilience Facility of the European Union within the framework of Programme Széchenyi Plan Plus.

#### Appendix A. Supplementary data

Supplementary data to this article can be found online at <https://doi.org/10.1016/j.apr.2025.102579>.

#### References

- Beobide, A., Moschovi, A., Mathioudakis, G., Kourtelesis, M., Lada, Z., Andrikopoulos, K., Sygellou, L., Dracopoulos, V., Yakoumis, I., Voyiatzis, G., 2022. High catalytic efficiency of a nanosized copper-based catalyst for automobiles: a physicochemical characterization. *Molecules* 27. <https://doi.org/10.3390/molecules27217402>.
- Bin, X., Yufeng, C., Yujuan, Z., Bangsheng, Z., Guiqing, L., Qian, L., Yang, Y., Tao, J., 2022. A review of recovery of palladium from the spent automobile catalysts. *Metals* 12, 1–20.
- Bourges, P., Lunati, S., Mabilon, G., 1998. N<sub>2</sub>O and NO<sub>2</sub> formation during NO reduction on precious metal catalysts. In: Kruse, N., Frennet, A., Bastin, J.-M. (Eds.), *Catalysis and Automotive Pollution Control IV, Studies in Surface Science and Catalysis*. Elsevier, pp. 213–222. [https://doi.org/10.1016/S0167-2991\(98\)80878-1](https://doi.org/10.1016/S0167-2991(98)80878-1).
- Choya, A., Rivas, B., González-Velasco, J., Gutierrez-Ortiz, J.I., Lopez-Fonseca, R., 2021. Optimisation of bimetallic Co-Ni supported catalysts for oxidation of methane in natural gas vehicles. *Appl. Catal. B Environ.* 284, 119712. <https://doi.org/10.1016/j.apcatb.2020.119712>.
- Choya, A., Rivas, B., Gutierrez-Ortiz, J.I., Lopez-Fonseca, R., 2022. Beneficial effects of nickel promoter on the efficiency of alumina-supported Co<sub>3</sub>O<sub>4</sub> catalysts for lean methane oxidation. *J. Environ. Chem. Eng.* 10, 108816. <https://doi.org/10.1016/j.jece.2022.108816>.
- Darby, M., Sykes, C., Michaelides, A., Stamatakis, M., 2018. Carbon monoxide poisoning resistance and structural stability of single atom alloys. *Top. Catal.* 61. <https://doi.org/10.1007/s11244-017-0882-1>.
- Després, J., Elsener, M., Koebel, M., Kröcher, O., Schnyder, B., Wokaun, A., 2004. Catalytic oxidation of nitrogen monoxide over Pt/SiO<sub>2</sub>. *Appl. Catal. B Environ.* 50, 73–82. <https://doi.org/10.1016/j.apcatb.2003.12.020>.
- Ding, J.C., Zhang, T.F., Mane, R.S., Kim, K.-H., Kang, M.C., Zou, C.W., Wang, Q.M., 2018. Low-temperature deposition of nanocrystalline Al<sub>2</sub>O<sub>3</sub> films by ion source-assisted magnetron sputtering. *Vacuum* 149, 284–290. <https://doi.org/10.1016/j.vacuum.2018.01.009>.
- Farahmandjou, M., Nazafarin, G., 2015. New pore structure of nano-alumina (Al<sub>2</sub>O<sub>3</sub>) prepared by sol gel method. *J. Ceram. Process. Res.* 16 (2), 237–240.
- Graham, G., Jen, H., Ezekoye, O., Kudla, R., Chun, W., Pan, X., McCabe, R., 2007. Effect of alloy composition on dispersion stability and catalytic activity for NO oxidation

- over alumina-supported Pt–Pd catalysts. *Catal. Lett.* 116, 1–8. <https://doi.org/10.1007/s10562-007-9124-7>.
- Guczi, L., Boskovic, G., Kiss, E., 2010. Bimetallic cobalt based catalysts. *Catal. Rev. Eng. - CATAL REV-SCI ENG* 52, 133–203. <https://doi.org/10.1080/01614941003720134>.
- Kim, C., Schmid, M., Schmieg, S., Tan, J., Li, W., 2011. The effect of Pt-Pd ratio on oxidation catalysts under simulated diesel exhaust. *SAE Tech. Pap.* <https://doi.org/10.4271/2011-01-1134>.
- Kim, J., Kwon, D.W., Lee, S., Ha, H.P., 2018. Exploration of surface properties of Sb-promoted copper vanadate catalysts for selective catalytic reduction of NOx by NH<sub>3</sub>. *Appl. Catal. B Environ.* 236, 314–325. <https://doi.org/10.1016/j.apcatb.2018.05.024>.
- Li, R., Zhu, Y., Zhang, Z., Zhang, C., Fu, G., Yi, X., Huang, Q., Yang, F., Liang, W., Zheng, A., Jiang, J., 2021. Remarkable performance of selective catalytic reduction of NOx by ammonia over copper-exchanged SSZ-52 catalysts. *Appl. Catal. B Environ.* 283, 119641. <https://doi.org/10.1016/j.apcatb.2020.119641>.
- Lin, L.-C., Kuo, C.-H., Hsu, Y.-H., Hsu, L.-C., Chen, H.-Y., Chen, J.-L., Pan, Y.-T., 2022. High-Performance intermetallic PtCo oxygen reduction catalyst promoted by molybdenum. *Appl. Catal. B Environ.* 317, 121767. <https://doi.org/10.1016/j.apcatb.2022.121767>.
- Liu, L., Corma, A., 2023. Bimetallic sites for catalysis: from binuclear metal sites to bimetallic nanoclusters and nanoparticles. *Chem. Rev.* 123, 4855–4933. <https://doi.org/10.1021/acs.chemrev.2c00733>.
- Meng, F., Yang, M., Li, Z., Zhang, R., 2020. HCOOH dissociation over the Pd-Decorated Cu bimetallic catalyst: the role of the Pd ensemble in determining the selectivity and activity. *Appl. Surf. Sci.* 511, 145554. <https://doi.org/10.1016/j.apsusc.2020.145554>.
- Michalek, T., Hessel, V., Wojnicki, M., 2024. Production, recycling and economy of palladium: a critical review. *Materials* 17, 1–20. <https://doi.org/10.3390/ma17010045>.
- Nazarpoor, Z., Golden, S.J., 2016. Bimetallic synergized PGM catalyst systems for TWC application. *World Pat* 2.
- Nkuna, R., Ijoma, G., Matambo, T., 2022. Accessing metals from low-grade ores and the environmental impact considerations: a review of the perspectives of conventional versus bioleaching strategies. *Minerals* 12, 506. <https://doi.org/10.3390/min12050506>.
- Padamata, S.K., Yasinskiy, A., Polyakov, P., Pavlov, E., Varyukhin, D., 2020. Recovery of noble metals from spent catalysts: a review. *Metall. Mater. Trans. B.* <https://doi.org/10.1007/s11663-020-01913-w>.
- Peckmann, C.H., 2021. Copper and Noble Metal Polymetallic Catalysts for Engine Exhaust Gas Treatment, vol. 1, pp. 1–21.
- Qi, F., Peng, J., Liang, Z., Guo, J., Liu, J., Fang, T., Mao, H., 2024. Strong metal-support interaction (SMSI) in environmental catalysis: mechanisms, application, regulation strategies, and breakthroughs. *Environ. Sci. Ecotechnol.* 22, 100443. <https://doi.org/10.1016/j.ese.2024.100443>.
- Rezaei, R., Moradi, G., 2018. Study of the performance of dry methane reforming in a microchannel reactor using sputtered Ni/Al<sub>2</sub>O<sub>3</sub> coating on stainless steel. *Int. J. Hydrogen Energy* 43, 21374–21385. <https://doi.org/10.1016/j.ijhydene.2018.09.200>.
- Robles-Lorite, L., Dorado, R., Torres-Jimenez, E., Bombek, G., Lešnik, L., 2023. Recent advances in the development of automotive catalytic converters: a systematic review. *Energies* 16, 6425. <https://doi.org/10.3390/en16186425>.
- Salaev, M., Kulchakovskaya, E., Vodyankina, O., 2022. Bimetallic Ag-based catalysts for low-temperature SCR: quo vadis? *Appl. Catal. Gen.* 644, 118815. <https://doi.org/10.1016/j.apcata.2022.118815>.
- Salaev, M., Salaeva, A.A., Kharlamova, T., Mamontov, G., 2021. Pt–CeO<sub>2</sub>-based composites in environmental catalysis: a review. *Appl. Catal. B Environ.* 295, 120286. <https://doi.org/10.1016/j.apcatb.2021.120286>.
- Uddin, M.N., Wang, F., 2024. Fuelling a clean future: a systematic review of techno-economic and life cycle assessments in E-Fuel development. *Appl. Sci.* 14. <https://doi.org/10.3390/app14167321>.
- Xing, F., Jeon, J., Toyao, T., Shimizu, K., Furukawa, S., 2019. Cu–Pd single-atom alloy catalyst for highly efficient NO reduction. *Chem. Sci.* 10. <https://doi.org/10.1039/C9SC03172C>.
- Xiong, J., Yang, J., Chi, X., Wu, K., Song, L., Li, T., Zhao, Y., Huang, H., Chen, P., Wu, J., Chen, L., Fu, M., Ye, D., 2021. Pd-Promoted Co<sub>2</sub>NiO<sub>4</sub> with lattice Co–O–Ni and interfacial Pd–O activation for highly efficient methane oxidation. *Appl. Catal. B Environ.* 292, 120201. <https://doi.org/10.1016/j.apcatb.2021.120201>.
- Yadav, G., Singh, A., Dutta, A., Uekert, T., DesVeaux, J.S., Nicholson, S.R., Tan, E.C.D., Mukarakate, C., Schaidle, J.A., Wrasman, C.J., Carpenter, A.C., Baldwin, R.M., Román-Leshkov, Y., Beckham, G.T., 2023. Techno-economic analysis and life cycle assessment for catalytic fast pyrolysis of mixed plastic waste. *Energy Environ. Sci.* 16, 3638–3653. <https://doi.org/10.1039/d3ee00749a>.
- Zhong, L., Barreau, M., Caps, V., Papaefthimiou, V., Haevecker, M., Teschner, D., Baaziz, W., Borfecchia, E., Braglia, L., Zafeiratos, S., 2021a. Improving the catalytic performance of cobalt for CO preferential oxidation by stabilizing the active phase through vanadium promotion. *ACS Catal.* 11, 5369–5385. <https://doi.org/10.1021/acscatal.0c05482>.
- Zhong, L., Barreau, M., Chen, D., Caps, V., Haevecker, M., Teschner, D., Simonne, D., Borfecchia, E., Baaziz, W., Šmíd, B., Zafeiratos, S., 2021b. Effect of manganese promotion on the activity and selectivity of cobalt catalysts for CO preferential oxidation. *Appl. Catal. B Environ.* 297, 120397. <https://doi.org/10.1016/j.apcatb.2021.120397>.
- Zhou, S., Lu, C., Yi, B., Zhou, C., Li, Q., Tan, L., Dong, L., 2023. Selective hydrogenation of acetylene on carbon-encapsulated ni-co-cu trimetallic nanoparticles: synergizing electronic effects and spatial confinement. *Chem. Eng. J.* 476, 146594. <https://doi.org/10.1016/j.cej.2023.146594>.
- Zou, X., Rui, Z., Ji, H.-B., 2017. Core-shell NiO@PdO nanoparticles supported on alumina as an advanced catalyst for methane oxidation. *ACS Catal.* 7. <https://doi.org/10.1021/acscatal.6b03105>.